

## Color collective effects at the early stage of ultrarelativistic heavy-ion collisions

Stanisław Mrówczyński\*

*High-Energy Department, Soltan Institute for Nuclear Studies, ul. Hoża 69, PL-00-681 Warsaw, Poland*

(Received 20 September 1993)

Hard and semihard processes lead to a copious production of partons at the early stage of ultrarelativistic heavy-ion collisions. Since the parton momentum distribution is strongly anisotropic, the system can be unstable with respect to the specific plasma modes. The conditions of instability are found and the characteristic time of its development is estimated. Then, the screening of the static chromoelectric field in the nonequilibrium plasma is studied. Importance of the two phenomena for heavy-ion collisions at the Brookhaven Relativistic Heavy Ion Collider and the CERN Large Hadron Collider is critically discussed.

PACS number(s): 12.38.Mh, 25.75.+r

### I. INTRODUCTION

A copious production of partons, mainly gluons, due to hard and semihard processes is expected in ultrarelativistic heavy-ion collisions [1–10]. For example, the number of gluons generated at the early stage of the central Au-Au collision is estimated [6] as 570 at the Brookhaven Relativistic Heavy Ion Collider (RHIC) ( $\sqrt{s} = 200$  GeV per  $N$ - $N$  collision) and 8100 at the CERN Large Hadron Collider (LHC) ( $\sqrt{s} = 6$  TeV per  $N$ - $N$  collision). Since the nucleons from the initial state are colorless, one usually assumes that the produced many-parton system is not only globally but also locally colorless,<sup>1</sup> and consequently collective effects due to the color degrees of freedom are neglected when the temporal evolution of the system is studied [7–9]. The local color neutrality can be obviously violated by random color fluctuations. Their role, however, is not very important if the fluctuations are effectively damped and the local neutrality is restored fast. This is the case of the plasma which is close to the thermodynamical equilibrium [11–13]. When the momentum distribution of partons is strongly anisotropic, as happens at the early stage of ultrarelativistic heavy-ion collisions, one expects, in analogy to the electron-ion plasma case [11], an existence of the unstable plasma modes with amplitudes exponentially growing in time. Then the system dynamics is dominated by the mean-field interaction and its behavior is essentially collective.

The main goal of this study is to show that the many-parton system generated at the early stage of ultrarelativistic heavy-ion collisions is indeed unstable with respect to the plasma modes. We use the methods of the electron-ion plasma physics [11] within a framework of the quark-gluon transport theory [12,13]. The quark-gluon plasma is assumed to be perturbative, i.e., weakly

interacting. We believe that such an assumption can be justified in the following way.

When hadrons collide only hard parton-parton interactions, those with the momentum transfer much greater than the QCD scale parameter  $\Lambda_{\text{QCD}} \cong 0.2$  GeV, can be treated in a perturbative way. One usually models soft nonperturbative interactions assuming existence of the colorless strings or clusters, which further decay into hadrons. When numerous partons are produced and their density  $\rho$  is so large that  $\rho^{1/3} \gg \Lambda_{\text{QCD}}$ , the asymptotic freedom regime is presumably approached due to the screening of color forces and then even soft parton interactions can be treated in a perturbative way. Therefore the strings or colorless clusters are expected to dissolve into partons. Then the transverse momentum cutoff which separates the perturbative from nonperturbative domain should be reduced.

In that way we have arrived at the second goal of this study, which is the color screening. Specifically, we compute the screening lengths of the static chromoelectric field in the nonequilibrium plasma, which have been briefly discussed in [6]. These lengths appear to be smaller than the confinement scale  $\Lambda_{\text{QCD}}^{-1}$ . Therefore the perturbative analysis seems to be plausible.

The results of this study have been earlier partially published [14]. This paper, which, except for some new results, gives a more systematic and detailed presentation, is organized as follows. In Sec. II we formulate the objectives of our considerations. Using the so-called Penrose criterion [11], we discuss the stability conditions in Sec. III. The next section presents an explicit unstable solution of the dispersion equation. In Sec. V the characteristic time of the instability development is estimated and the relevance of our findings to heavy-ion collisions at RHIC and LHC is discussed. The discussion of the color screening is given in Sec. VI. At the end we summarize our considerations and speculate about possible experimental consequences of our findings.

### II. DISPERSION EQUATION

The spectrum of plasma modes, which reflect the collective behavior of the system, is determined by the dis-

\*Electronic address: MROW@PLEARN.bitnet

<sup>1</sup>We call a system locally colorless when not only the color charge, but also the color current, vanishes as well.

persion equation. As has been shown within the kinetic theory of the quark-gluon plasma [12,13], the dispersion equation of the (small) plasma oscillations in the anisotropic system coincides with that one of the electrodynamic plasma and reads [13,15]

$$\det |\mathbf{k}^2 \delta^{ij} - k^i k^j - \omega^2 \epsilon^{ij}(\omega, \mathbf{k})| = 0, \quad i, j = x, y, z, \quad (2.1)$$

where  $\mathbf{k}$  is the wave vector and  $\omega$  is the frequency.  $\epsilon^{ij}$  is the chromodielectric tensor, which in the collisionless limit (see below) is

$$\begin{aligned} \epsilon^{ij}(\omega, \mathbf{k}) = & \delta^{ij} + \frac{2\pi\alpha_s}{\omega} \int \frac{d^3p}{(2\pi)^3} \frac{v^i}{\omega - \mathbf{k} \cdot \mathbf{v} + i0^+} \frac{\partial n(\mathbf{p})}{\partial p^j} \\ & \times \left[ \left( 1 - \frac{\mathbf{k} \cdot \mathbf{v}}{\omega} \right) \delta^{lj} + \frac{k^l v^j}{\omega} \right], \end{aligned} \quad (2.2)$$

where  $\alpha_s$  is the strong coupling constant and

$$n(\mathbf{p}) \equiv n_q(\mathbf{p}) + \bar{n}_q(\mathbf{p}) + 6n_g(\mathbf{p}), \quad (2.3)$$

with  $n_q$ ,  $\bar{n}_q$ , and  $n_g$  being the distribution function of quarks, antiquarks, and gluons normalized in such a way that the quark and gluon densities are

$$\rho_q = 3 \int \frac{d^3p}{(2\pi)^3} n_q(\mathbf{p}), \quad \rho_g = 8 \int \frac{d^3p}{(2\pi)^3} n_g(\mathbf{p}).$$

The quarks and gluons are assumed to be massless, and consequently the parton velocity  $\mathbf{v}$  equals  $\mathbf{p}/|\mathbf{p}|$ . The plasma is locally colorless, homogeneous, but not isotropic. It should be also stressed that in spite of the similarity to the electrodynamic formulas, Eqs. (2.1) and (2.2) take into account the essential non-Abelian effect, i.e., the gluon-gluon coupling [13].

We discuss the dispersion equation (2.1) in the collisionless limit, where the mean-field interaction is assumed to dominate the system dynamics. The assumption is correct if the inverse characteristic time of the mean-field phenomena,  $\tau^{-1}$ , is substantially larger than the collision frequency  $\nu$ . Otherwise, the infinitesimally small imaginary quantity  $i0^+$  from Eq. (2.2) should be substituted by  $i\nu$ . Such a substitution, however, seriously complicates analysis of the dispersion equation (2.1). Therefore we solve the problem within the collisionless limit and only *a posteriori* argue validity of this approximation.

The dielectric tensor (2.2) and consequently the solutions of Eq. (2.1) are fully determined by the parton momentum distribution, which we assume to be the same for quarks and gluons. In the further discussion, we consider two forms of the distribution function

$$n(y, p_\perp, \phi) = \frac{1}{2Y} \Theta(Y - y) \Theta(Y + y) h(p_\perp) \frac{1}{p_\perp \cosh y} \quad (2.4a)$$

and

$$n(p_\parallel, p_\perp, \phi) = \frac{1}{2\mathcal{P}_\parallel} \Theta(\mathcal{P}_\parallel - p_\parallel) \Theta(\mathcal{P}_\parallel + p_\parallel) h(p_\perp), \quad (2.4b)$$

where  $y$ ,  $p_\parallel$ ,  $p_\perp$ , and  $\phi$  denote parton rapidity, longitudinal and transverse momenta, and azimuthal angle, respectively. Equation (2.4a) gives the parton number distribution ( $dN/d^2p_\perp dy$ ), which is flat in the rapidity interval  $(-Y, Y)$ , while the parton number distribution ( $dN/d^2p_\perp dp_\parallel$ ) corresponding to Eq. (2.4b) is flat in the longitudinal momentum interval  $(-\mathcal{P}_\parallel, \mathcal{P}_\parallel)$ . We will further refer to Eqs. (2.4a) and (2.4b) as the flat  $y$  and flat  $p_\parallel$  distributions, respectively.

The solutions  $\omega(\mathbf{k})$  of Eq. (2.1) are stable when  $\text{Im}\omega < 0$  and unstable when  $\text{Im}\omega > 0$ . In the first cases, the amplitude exponentially decreases in time, while in the second one there is an exponential growth. In practice, it appears difficult to find solutions of Eq. (2.1) because of the complicated structure of the chromodielectric tensor (2.2). However, the stability analysis can be performed without solving Eq. (2.1) explicitly.

### III. UNSTABLE CONFIGURATION AND PENROSE CRITERION

When the momentum distribution is a monotonously decreasing function of  $|\mathbf{p}|$ , as is the case of (2.4), the longitudinal modes, those with the wave vector  $\mathbf{k}$  parallel to the chromoelectric field  $\mathbf{E}$ , are stable [11]. Thus one should look for instabilities among transversal modes. When the instability occurs, the kinetic energy of particles is converted into the field energy. Since the energy of the parton motion along the beam direction, which we identify with the  $z$  axis, exceeds the perpendicular energy, the instability is expected to appear when the chromoelectric field is along the  $z$  axis while the wave vector is transversal to it. Thus we will consider the configuration

$$\mathbf{E} = (0, 0, E), \quad \mathbf{k} = (k, 0, 0). \quad (3.1)$$

Let us mention that the unstable mode, the so-called filamentation instability, has been just found for this configuration in the two-stream system of the quark-gluon plasma [15,16]. As we shall briefly discuss at the end of the next section, the instability studied here also provides the characteristic pattern with the filaments along the beam with the color currents of the opposite sign in the neighboring filaments. It is also interesting to note that the electron-ion plasma from the pinch experiments is "hotter" in the transverse direction (due to magnetic squeezing) and then the instability appears in the configuration where the electric field is perpendicular and the wave vector longitudinal to the pinch axis.

With the configuration (3.1), the dispersion equation (2.1) simplifies to

$$H(\omega) \equiv k^2 - \omega^2 \epsilon^{zz}(\omega, k) = 0, \quad (3.2)$$

where only one diagonal component of the dielectric tensor enters.

The Penrose criterion states that *the dispersion equation  $H(\omega) = 0$  has unstable solutions if  $H(\omega = 0) < 0$*  [11]. The meaning of this statement will be clearer after we will approximately solve the dispersion equation in

the next section.

Let us compute  $H(0)$ , which can be written as

$$H(0) = k^2 - \chi^2, \quad (3.3)$$

with

$$\chi^2 \equiv -\omega_0^2 - 2\pi\alpha_s \int \frac{d^3p}{(2\pi)^3} \frac{v_z^2}{v_x} \frac{\partial n(\mathbf{p})}{\partial p_x}, \quad (3.4)$$

where the plasma frequency parameter is

$$\omega_0^2 \equiv -2\pi\alpha_s \int \frac{d^3p}{(2\pi)^3} v_z \frac{\partial n(\mathbf{p})}{\partial p_z}. \quad (3.5)$$

As we shall see below,  $\omega_0$  gives the frequency of the stable mode of the configuration (3.1) when  $k \rightarrow 0$ .

Substituting the distribution functions (2.4) into Eqs. (3.4) and (3.5), one finds the analytical but rather complicated expression of  $H(0)$ . In the case of the flat  $y$  distribution, we thus take the limit  $\cosh Y \gg 1$ , while for the flat  $p_{\parallel}$  distribution we assume that  $\langle p_{\parallel} \rangle \gg \langle p_{\perp} \rangle$ , where  $\langle p_{\parallel, \perp} \rangle$  is the average longitudinal or transverse momentum. Both limits are obviously satisfied in the ultra-relativistic heavy-ion collisions. Then we get

$$\chi^2 \cong -\frac{\alpha_s}{4\pi} \frac{e^Y}{Y} \int dp_{\perp} \left( h(p_{\perp}) + p_{\perp} \frac{dh(p_{\perp})}{dp_{\perp}} \right) \quad (3.6a)$$

for the flat  $y$  distribution and

$$\chi^2 \cong -\frac{\alpha_s}{4\pi} \mathcal{P}_{\parallel} \int dp_{\perp} \frac{dh(p_{\perp})}{dp_{\perp}} \quad (3.6b)$$

for the flat  $p_{\parallel}$  distribution.

After performing partial integrations in Eqs. (3.6), these equations can be rewritten as

$$\chi^2 \cong \frac{\alpha_s}{4\pi} \frac{e^Y}{Y} p_{\perp}^{\min} h(p_{\perp}^{\min}), \quad (3.7a)$$

$$\chi^2 \cong \frac{\alpha_s}{4\pi} \mathcal{P}_{\parallel} h(p_{\perp}^{\min}), \quad (3.7b)$$

where  $p_{\perp}^{\min}$  is the minimal transverse momentum and the function  $h(p_{\perp})$  is assumed to decrease faster than  $1/p_{\perp}$  when  $p_{\perp} \rightarrow \infty$ .

As seen, the sign of  $H(0)$  given by Eq. (3.3) is (for sufficiently small  $k^2$ ) determined by the transverse momentum distribution at the minimal momentum. There are unstable modes (3.1) if  $p_{\perp}^{\min} h(p_{\perp}^{\min}) > 0$  for the flat  $y$  distribution and if  $h(p_{\perp}^{\min}) > 0$  for the flat  $p_{\parallel}$ -distribution.

Since the transverse momentum distribution  $h(p_{\perp})$  is expected to be a monotonously decreasing function of  $p_{\perp}$ , the instability condition for the flat  $p_{\parallel}$  distribution seems to be always satisfied. The situation with the flat  $y$  distribution is less clear. So let us discuss it in more detail. We consider three characteristic cases of  $h(p_{\perp})$  discussed in the literature.

(1) The transverse momentum distribution due to a single binary parton-parton interaction is proportional to  $p_{\perp}^{-6}$  [2] and blows up when  $p_{\perp} \rightarrow 0$ . In such a case  $p_{\perp}^{\min} h(p_{\perp}^{\min}) > 0$ , there are unstable modes and  $p_{\perp}^{\min}$  should be treated as a cutoff parameter reflecting, e.g.,

the finite size of the system.

(2) The transverse momentum distribution proportional to  $(p_{\perp} + m_{\perp})^{-6.4}$  with  $m_{\perp} = 2.9$  GeV has been found in [6], where except binary parton-parton scattering the initial and final state radiation has been taken into account. This distribution, in contrast to that from (1), gives  $p_{\perp}^{\min} h(p_{\perp}^{\min}) = 0$  for  $p_{\perp}^{\min} = 0$ , and there is no instability, although one should remember that the finite value of  $m_{\perp}$  found in [6] is the result of infrared cutoff parameters used when  $h(p_{\perp})$  has been computed. Thus it seems more reasonable to use the distribution from (1), where the cutoff explicitly appears.

(3) One treats perturbatively only partons with  $p_{\perp} > p_{\perp}^{\min}$  assuming that those with lower momenta form colorless clusters or strings due to a nonperturbative interaction. It should be stressed that the colorless objects do not contribute to the dielectric tensor (2.2), which is found in the linear response approximation [12–14]. Thus only the partons with  $p_{\perp} > p_{\perp}^{\min}$  are of interest for us. Consequently,  $p_{\perp}^{\min} h(p_{\perp}^{\min})$  is positive and there are unstable modes. It will be shown in Sec. VI that the screening lengths due to the large parton density are smaller than the confinement scale in the vacuum. Therefore, as discussed in the Introduction, the cutoff parameter  $p_{\perp}^{\min}$  should be presumably reduced from 1–2 GeV usually used for proton-proton interactions to, let us say, 0.1–0.2 GeV.

We cannot draw a firm conclusion, but we see that the instability condition is trivially satisfied for the flat  $p_{\parallel}$  distribution and is also fulfilled for the flat  $y$  distribution under plausible assumptions. Let us mention that the difference between the instability conditions for the flat  $y$  and  $p_{\parallel}$  distributions is due to a very specific property of the  $y$  distribution which is limited to the interval  $(-Y, Y)$ . The point is that  $y \rightarrow \pm\infty$  when  $p_{\perp} \rightarrow 0$ , and consequently, the limits in the rapidity suppress the contribution from the small transverse momenta to the dielectric tensor. For this reason we need for the instability the distribution  $h(p_{\perp})$  which diverges for  $p_{\perp} \rightarrow 0$  in the case of the flat  $y$  distribution, while the instability condition for the flat  $p_{\parallel}$  distribution is satisfied when  $h(0)$  is finite. If we assumed the Gaussian rapidity distribution instead of (2.4a), the instability condition would be less stringent.

In any case, we assume that the Penrose criterion is satisfied and we look for the unstable modes solving the dispersion equation (3.2).

#### IV. SOLVING THE DISPERSION EQUATION

The dispersion equation (3.2) for a cylindrically symmetric system is

$$k^2 - \omega^2 + \omega_0^2 - \frac{\alpha_s}{4\pi^2} \int_0^{\infty} dp_{\perp} \int_{-\infty}^{\infty} dp_{\parallel} \frac{p_{\parallel}^2}{\sqrt{p_{\parallel}^2 + p_{\perp}^2}} \frac{\partial n}{\partial p_{\perp}} \times \int_0^{2\pi} \frac{d\phi \cos \phi}{a - \cos \phi + i0^+} = 0, \quad (4.1)$$

with the plasma frequency  $\omega_0$  given by Eq. (3.4) and  $a$  denoting

$$a \equiv \frac{\omega}{k} \frac{\sqrt{p_{\parallel}^2 + p_{\perp}^2}}{p_{\perp}}.$$

We solve Eq. (4.1) in the two limiting cases  $|\omega/k| \gg 1$  and  $|k/\omega| \gg 1$ . In the first case, the azimuthal integral is approximated as

$$\int_0^{2\pi} \frac{d\phi \cos \phi}{a - \cos \phi + i0^+} = \frac{\pi}{a^2} + O(a^{-4}).$$

Then Eq. (4.1) gets the form

$$k^2 - \omega^2 + \omega_0^2 + \eta^2 \frac{k^2}{\omega^2} = 0, \quad (4.2)$$

where  $\eta$ , as  $\omega_0$ , is a constant defined as

$$\eta_0^2 \equiv -\frac{\alpha_s}{4\pi} \int dp_{\parallel} dp_{\perp} \frac{p_{\parallel}^2 p_{\perp}^2}{(p_{\parallel}^2 + p_{\perp}^2)^{3/2}} \frac{\partial n(\mathbf{p})}{\partial p_{\perp}}.$$

We have computed  $\omega_0$  and  $\eta$  for the flat  $p_{\parallel}$  and  $y$  distributions. In the limit  $\cosh Y \gg 1$  and  $\langle p_{\parallel} \rangle \gg \langle p_{\perp} \rangle$ , respectively, we have found

$$\omega_0^2 \cong \frac{\alpha_s}{8Y} \int dp_{\perp} h(p_{\perp}), \quad (4.3a)$$

$$\omega_0^2 \cong \frac{\alpha_s}{2\pi \mathcal{P}_{\parallel}} \int dp_{\perp} p_{\perp} h(p_{\perp}) \quad (4.3b)$$

and

$$\eta^2 \cong \frac{\alpha_s}{16Y} \int dp_{\perp} \left( \frac{1}{4} h(p_{\perp}) - p_{\perp} \frac{dh(p_{\perp})}{dp_{\perp}} \right), \quad (4.4a)$$

$$\eta^2 \cong -\frac{\alpha_s}{4\pi \mathcal{P}_{\parallel}} \ln \left( \frac{\mathcal{P}_{\parallel}}{\langle p_{\perp} \rangle} \right) \int dp_{\perp} p_{\perp}^2 \frac{dh(p_{\perp})}{dp_{\perp}}. \quad (4.4b)$$

The solutions of Eq. (4.2) are

$$\omega_{\pm}^2 = \frac{1}{2}(k^2 + \omega_0^2 \pm \sqrt{(k^2 + \omega_0^2)^2 + 4\eta^2 k^2}).$$

One sees that  $\omega_+^2 \geq 0$  and  $\omega_-^2 \leq 0$ . Thus there is a pure real mode  $\omega_+$ , which is stable, and two pure imaginary modes  $\omega_-$ , one of them being unstable. As mentioned previously,  $\omega_+ = \omega_0$  when  $k = 0$ .

Let us focus our attention on the unstable mode, which can be approximated as

$$\omega_-^2 \cong \begin{cases} -\frac{\eta^2}{\omega_0^2} k^2 & \text{for } k^2 \ll \omega_0^2, \\ -\eta^2 & \text{for } k^2 \gg \omega_0^2. \end{cases} \quad (4.5)$$

One should keep in mind that Eq. (4.5) holds only for  $|\omega/k| \gg 1$ . We see that  $\omega_-$  can satisfy this condition for  $k^2 \ll \omega_0^2$  if  $\eta^2 \gg \omega_0^2$  and for  $k^2 \gg \omega_0^2$  if  $\eta^2 \ll \omega_0^2$ .

To check whether these conditions can be satisfied, we compare  $\eta^2$  to  $\omega_0^2$ . Assuming that  $h(p_{\perp}) \sim p_{\perp}^{-\beta}$ , one finds, from Eqs. (4.3) and (4.4),

$$\eta^2 \cong \frac{1 + 4\beta}{8} \omega_0^2. \quad (4.6a)$$

$$\eta^2 \cong \frac{\beta}{2} \ln \left( \frac{\mathcal{P}_{\parallel}}{\langle p_{\perp} \rangle} \right) \omega_0^2. \quad (4.6b)$$

Since  $\beta \cong 6$  [2,6], we get  $\eta^2 \geq 3\omega_0^2$ . Therefore the solution (4.5) for  $k^2 \ll \omega_0^2$  should be correct.

Let us now solve the dispersion equation (4.1) in the second case when  $|k/\omega| \gg 1$ . Then the azimuthal integral from Eq. (4.1) is approximated as

$$\int_0^{2\pi} \frac{d\phi \cos \phi}{a - \cos \phi + i0^+} = -2\pi + O(a),$$

and we immediately get the dispersion relation

$$\omega^2 = k^2 - \chi^2, \quad (4.7)$$

with  $\chi^2$  given by Eq. (3.6) or (3.7). As previously, we have assumed that  $\cosh Y \gg 1$  and  $\langle p_{\parallel} \rangle \gg \langle p_{\perp} \rangle$ . Equation (4.7) provides a real mode for  $k^2 > \chi^2$  and two imaginary modes for  $k^2 < \chi^2$ . Since the solution (4.7) must satisfy the condition  $|k/\omega| \gg 1$ , it holds only for  $k^2 \gg |k^2 - \chi^2|$ .

The dispersion relation of the unstable mode in the whole domain of wave vectors is schematically shown in Fig. 1, where the solutions (4.5) and (4.7) are combined. Now one sees how the Penrose criterion works. When  $\chi^2 = 0$ , the unstable mode disappears.

Using the Maxwell equations, one easily finds the space-time structure of the instability. It starts when a fluctuation generates a small color current along the beam. If this current changes in the transverse direction at a length which is greater than  $\chi^{-1}$ , the fluctuation grows and the initially colorless system splits into the filaments of thickness  $\pi/k$ , where  $k$  is the wave vector, with the color current flowing in the opposite directions in the neighboring filaments. Unfortunately, the linear response analysis performed here does not allow one to follow the instability development beyond the moment when the deviation from the color neutrality is large.

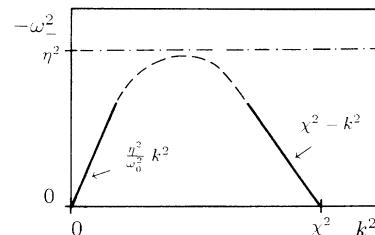


FIG. 1. Schematic view of the dispersion relation of the unstable mode.

More specifically, the distribution function  $n' = n + \delta n$ , which describes the deviation from the colorless state  $n$ , must satisfy the condition  $|n| \gg |\delta n|$  [13].

### V. CAN THE INSTABILITY OCCUR IN HEAVY-ION COLLISIONS?

The instability studied here is relevant to the heavy-ion collisions if the time of instability development is short enough, shorter than the characteristic time of evolution of the nonequilibrium state described by the distribution function (2.4).

Let us first estimate the time of instability development which is given by  $1/\text{Im}\omega$ . As seen in Fig. 1,  $|\text{Im}\omega| < \eta$ . Thus we define the minimal time as  $\tau_{\min} = 1/\eta$ . To find  $\tau_{\min}$  we estimate the plasma frequency. We consider here only the flat  $y$  distribution, which seems to be more reasonable than the flat  $p_{\parallel}$  distribution. Approximating  $\int dp_{\perp} h(p_{\perp})$  as  $\int dp_{\perp} p_{\perp} h(p_{\perp}) / \langle p_{\perp} \rangle$ , the plasma frequency (4.3a) can be written as

$$\omega_0^2 \cong \frac{\alpha_s \pi}{6Y r_0^2 A^{2/3}} (N_q + N_{\bar{q}} + \frac{9}{4} N_g), \quad (5.1)$$

where  $N_q$ ,  $N_{\bar{q}}$ , and  $N_g$  are the number of quarks, anti-quarks, and gluons, respectively, produced in the volume, which has been estimated in the following way. Since we are interested in the central collisions, the volume corresponds to a cylinder of the radius  $r_0 A^{1/3}$  with  $r_0 = 1.1$  fm and  $A$  being the mass number of the colliding nuclei. Using the uncertainty principle argument, the length of the cylinder has been taken as  $1/\langle p_{\perp} \rangle$ , which is the formation time of partons with transverse momentum  $\langle p_{\perp} \rangle$ .

Neglecting quarks and antiquarks in Eq. (5.1) and substituting there  $N_g = 570$  for the central Au-Au collision at RHIC ( $Y = 2.5$ ) and  $N_g = 8100$  for the same colliding system at LHC ( $Y = 5.0$ ) [6], we get

$$\omega_0 = 280 \text{ MeV for RHIC, } \omega_0 = 430 \text{ MeV for LHC}$$

for  $\alpha_s = 0.3$  at RHIC and  $\alpha_s = 0.1$  at LHC. Using Eq. (4.6a) with  $\beta = 6$ , one finds

$$\begin{aligned} \tau_{\min} &= 0.4 \text{ fm/c for RHIC,} \\ \tau_{\min} &= 0.3 \text{ fm/c for LHC.} \end{aligned} \quad (5.2)$$

The plasma has been assumed to be collisionless in our analysis. Such an assumption is usually correct for weakly interacting systems because the damping rates of the collective modes due to collisions are of the higher order in  $\alpha_s$  than the frequencies of these modes; see, e.g., [13]. However, it has been argued recently [17] that the color collective modes are overdamped due to the unscreened chromomagnetic interaction. However, it is unclear whether these arguments concern the unstable mode discussed here. The point is that Ref. [17] deals with the neutralization of color charges which generate the longitudinal chromoelectric field, while the unstable mode, which we have found, is transversal and conse-

quently is generated by the color currents, not charges. Let us refer here once again to the electron-ion plasma, where the charge neutralization is a very fast process, while currents can exist in the system for a much longer time [11]. In any case, the above estimates of the instability development should be treated as lower limits.

Let us now discuss the characteristic time of evolution of the nonequilibrium state described by the distribution function (2.4). Except for the possible unstable collective modes, there are two other important processes responsible for the temporal evolution of the initially produced many-parton system: free streaming [18–20] and parton-parton scattering. The two processes lead to the isotropic momentum distribution of partons in a given space cell. The estimated time to achieve local isotropy due to the free streaming in the central slice of 1 fm width is about 0.7 fm/c at RHIC [20]. As one finds in Fig. 10(a) of Ref. [9] where the parton cascade was studied, the equilibrium is reached after about 1 fm/c at RHIC and about 0.5 fm/c at LHC. All estimates concern the central collisions of the heaviest nuclei. Thus the three time scales of interest are very similar to each other. Therefore the color unstable modes can play a role in the dynamics of a many-parton system produced at the early stage of a heavy-ion collision, but presumably the pattern of instability cannot fully develop.

Let us briefly discuss possible consequences of the instability. The growth of the color fluctuation, with the chromoelectric field along the beam and the wave vector perpendicular to it, leads to a conversion of the kinetic energy related to the parton motion along the beam to the transverse energy. It is known from electron-ion plasma studies that such an energy transport is very effective [11]. Thus the instability speeds up the equilibration process, leading to a more isotropic momentum distribution. One should keep in mind, however, that the collective modes discussed here are due to the mean-field interaction and that therefore they do not produce the entropy. Consequently, the instability contributes to the equilibration indirectly, reducing relative parton momenta and increasing the collision rate.

In contrast to the electron-ion plasma, the time of equilibration due to collisions is not much greater than the time of instability growth in the quark-gluon plasma. Therefore the instability contribution to the equilibration process is presumably not very large. The interplay between the instability development and equilibration needs further studies.

### VI. SCREENING

In this section we study screening of the static longitudinal chromoelectric field previously discussed in [6]. We consider the capacitor embedded in the quark-gluon plasma generated at the early stage of a nucleus-nucleus collision. Such a capacitor is a very simple model of the string where the chromoelectric field is spanned between the color charges at the string ends.

The field modification in the presence of the plasma is determined by the dielectric tensor (2.2). More specifically,

$$D^i(\omega, \mathbf{k}) = \epsilon^{ij}(\omega, \mathbf{k})E^j(\omega, \mathbf{k}), \quad i, j = x, y, z, \quad (6.1)$$

where  $D^i(\omega, \mathbf{k})$  is the Fourier transform of the chromoelectric induction, i.e., the chromoelectric field in the *perturbative* vacuum, while  $E^i(\omega, \mathbf{k})$  is the actual chromoelectric field. The color indices are suppressed in Eq. (6.1) since, as shown in [12,13], the dielectric tensor derived in the linear response approximation is proportional to the unit matrix in the color space. So there is no mixing of the field color components due to Eq. (6.1).

We further consider two situations: The capacitor field is along the beam ( $z$  axis), and the field is parallel to the  $x$  axis. Let us start with the first case. Then there is only a  $z$  component of the wave vector  $\mathbf{k} = (0, 0, k)$  and the Fourier transform of the induction vector is

$$D_z(\omega = 0, k) = E^0 \frac{2}{k} \sin \frac{kl}{2}, \quad (6.2)$$

where  $l$  is the distance between the capacitor plates which are located at  $z = l/2$  and  $z = -l/2$ ;  $E^0$  is the induction between the plates in coordinate space. Since the capacitor field is assumed to be static, only the zero-frequency component of the field is nonvanishing.

Let us now compute the dielectric tensor. We first observe that the distribution function (2.4) is symmetric with respect to the momentum inversion, i.e.,

$$n(\mathbf{p}) = n(-\mathbf{p}), \quad (6.3)$$

and consequently the momentum derivatives of the distribution function are antisymmetric. Then one easily shows that the off-diagonal components of the dielectric tensor  $\epsilon^{zx}$  and  $e^{zy}$  vanish and the dielectric tensor can be trivially inverted. It is essential here that there be only a  $k_z$  component of  $\mathbf{k}$  which is nonzero.

To take the limit  $\omega \rightarrow 0$  of  $\epsilon^{zz}(\omega, k)$ , one uses the identity

$$\frac{1}{\omega - kv_z} = -\frac{1}{kv_z} \sum_{n=0}^{\infty} \left( \frac{\omega}{kv_z} \right)^n$$

and observes that only the terms with odd  $n$  contribute to the integral because of the symmetry (6.3). Finally, one arrives to the result

$$\epsilon^{zz}(\omega = 0, k) = 1 + \frac{m_{\parallel}^2}{k^2}, \quad (6.4)$$

with

$$m_{\parallel}^2 \equiv -2\pi\alpha_s \int \frac{d^3p}{(2\pi)^3} \frac{1}{v_z} \frac{\partial n(\mathbf{p})}{\partial p_z}. \quad (6.5)$$

Substituting Eqs. (6.2) and (6.4) into Eq. (6.1), one finds the field after transforming it to coordinate space as

$$E_z(z) = \begin{cases} E^0 \exp\left(-\frac{m_{\parallel} l}{2}\right) \cosh(m_{\parallel} |z|) & \text{for } |z| < l/2, \\ -E^0 \exp(-m_{\parallel} |z|) \sinh\left(\frac{m_{\parallel} l}{2}\right) & \text{for } |z| > l/2, \end{cases} \quad (6.6)$$

which is illustrated in Fig. 2.

One sees that the capacitor field is modified in the plasma not only at finite distances from the plates, but at the plates as well. This differs from the screening of a point-like charge which is screened at finite distances  $r$  but the screening disappears when  $r \rightarrow 0$ . Let us also observe that  $E_z(z = l/2 - 0^+) - E_z(z = l/2 + 0^+) = E^0$ . This means that the charge collected at the plates is conserved.

When the capacitor field is parallel to the  $x$ -axis the wave vector  $\mathbf{k} = (k, 0, 0)$ , the only nonvanishing component of the dielectric tensor is  $\epsilon^{xx}$  and we get the result analogous to (6.6) with  $m_{\perp}$  instead of  $m_{\parallel}$ , which is

$$m_{\perp}^2 \equiv -2\pi\alpha_s \int \frac{d^3p}{(2\pi)^3} \frac{1}{v_x} \frac{\partial n(\mathbf{p})}{\partial p_x}. \quad (6.7)$$

Substituting the distribution functions (2.4) into (6.5) and (6.7) one computes the screening masses. In the limit  $\cosh Y \gg 1$  for the flat  $y$ -distribution (2.4a) and  $\langle p_{\parallel} \rangle \gg \langle p_{\perp} \rangle$  for the flat  $p_{\parallel}$ -distribution, respectively, we find

$$m_{\parallel}^2 \cong \frac{\alpha_s}{4Y} \int dp_{\perp} h(p_{\perp}), \quad (6.8a)$$

$$m_{\parallel}^2 \cong \frac{\alpha_s}{2\pi\mathcal{P}_{\parallel}} \int dp_{\perp} p_{\perp} h(p_{\perp}) \quad (6.8b)$$

and

$$m_{\perp}^2 \cong m_{\parallel}^2 + \frac{\alpha_s e^Y}{4\pi Y} p_{\perp}^{\min} h(p_{\perp}^{\min}), \quad (6.9a)$$

$$m_{\perp}^2 \cong \frac{\alpha_s}{4\pi} \mathcal{P}_{\parallel} h(p_{\perp}^{\min}). \quad (6.9b)$$

One sees that the transverse mass is very large for the unstable system [cf. Eq. (3.7a)]. This result is, however, rather meaningless. When the system is unstable and the transverse energy grows very fast, one cannot study the *static* screening in this direction.

Let us estimate the longitudinal screening length  $\lambda_{\parallel} = m_{\parallel}^{-1}$  for the flat  $y$  distribution. Repeating the considerations which led us to the estimate (5.2), we find

$$\lambda_{\parallel} = 0.5 \text{ fm for RHIC, } \lambda_{\parallel} = 0.3 \text{ fm for LHC.} \quad (6.10)$$

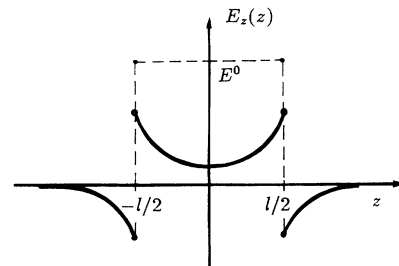


FIG. 2. Capacitor field modified in the plasma.

According to these estimates, which agree with those given in [6], the screening lengths are smaller than the confinement scale  $\Lambda_{\text{QCD}}^{-1}$ . Thus we can believe that the perturbative analysis is not senseless. The estimates (6.10) also suggest that strings of length  $l \cong 1$  fm have to dissolve in the plasma generated at the early stage of ultrarelativistic heavy-ion collisions.

It is instructive to compare the screening lengths (6.10) with the Debye screening length  $\lambda_D$  computed for the equilibrium gluon plasma at the temperature  $T$  (see, e.g., [12,13], which is

$$\lambda_D^{-2} = 4\pi\alpha_s T^2.$$

One finds that the screening lengths (6.10) correspond to the temperature about 0.2 GeV at RHIC and 0.6 GeV at LHC.

## VII. SUMMARY AND SOME SPECULATIONS

We have intended to show in this paper that in spite of the initial local colorlessness of the colliding system, specific color fluctuations can grow, leading a collective behavior of the many-parton system produced at the early stage of ultrarelativistic heavy-ion collisions. Using the Penrose criterion, we have found the instability condition and have argued that this condition is satisfied in heavy-ion collisions at RHIC or LHC. Then we have solved approximately the dispersion relation and have found explicitly the unstable mode. The development of such a mode leads to the characteristic filament structure of the color current. We have estimated the time of the instability growth, which seems to be somewhat smaller than the time needed to equilibrate the many-parton system due to the parton collisions or free streaming. Therefore

there is a chance that the instability can, at least to some extent, develop in heavy-ion collisions.

The quark-gluon plasma has been treated as a weakly interacting system in our analysis. We have showed that in spite of rather small values of the coupling constant  $\alpha_s$ , which we have been assumed (0.3 for RHIC and 0.1 for LHC), the screening lengths are smaller than the confinement scale  $\Lambda_{\text{QCD}}^{-1}$ . Thus the perturbative approach seems to be reasonable.

At the end, let us briefly speculate on possible experimental consequences of the plasma instability. Since the longitudinal energy is converted into transverse one when the instability grows, broadening of the transverse momentum distribution is expected. The instability initiates as a random color fluctuation. Thus there should be collisions where the unstable mode develops and collisions without this mode. The azimuthal orientation of the wave vector should also change from one collision to another. Therefore the instability is expected to produce significant fluctuations of the transverse momentum in a given phase space cell, in contrast to the parton cascade simulations [7–9], where fluctuations are strongly damped due to the large number of uncorrelated partons. The event-by-event analysis of the fluctuations might be a tool to observe experimentally the instability.

## ACKNOWLEDGMENTS

I am very grateful to B. Müller for the discussion on the screening lengths. This work was partially supported by Polish Committee of Scientific Research and Marie Curie Fund under Grants Nos. 20436-91-01 and MEN/DOE-92-87, respectively.

- 
- [1] K. Kajantie, P. V. Landshoff, and J. Lindfors, *Phys. Rev. Lett.* **59**, 2517 (1987).
  - [2] K. J. Eskola, K. Kajantie, and J. Lindfors, *Nucl. Phys.* **B323**, 37 (1989).
  - [3] J.-P. Blaizot and A. H. Mueller, *Nucl. Phys.* **B289**, 847 (1987).
  - [4] G. Calucci and D. Treleani, *Phys. Rev. D* **41**, 3367 (1990); **44**, 2746 (1991).
  - [5] X.-N. Wang and M. Gyulassy, *Phys. Rev. D* **44**, 3501 (1991); *Phys. Rev. Lett.* **68**, 1480 (1992).
  - [6] T. S. Biró, B. Müller, and X.-N. Wang, *Phys. Lett. B* **283**, 171 (1992).
  - [7] K. Geiger and B. Müller, *Nucl. Phys.* **B369**, 600 (1992).
  - [8] K. Geiger, *Phys. Rev. D* **46**, 4965 (1992); **47**, 133 (1993).
  - [9] K. Geiger, *Phys. Rev. D* **46**, 4986 (1992).
  - [10] E. Shuryak, *Phys. Rev. Lett.* **68**, 3270 (1987).
  - [11] N. A. Krall and A. W. Trivelpiece, *Principles of Plasma Physics* (McGraw-Hill, New York, 1973).
  - [12] H.-Th. Elze and U. Heinz, *Phys. Rep.* **183**, 81 (1989).
  - [13] St. Mrówczyński, in *Quark-Gluon Plasma*, edited by R. Hwa (World Scientific, Singapore, 1990); *Phys. Rev. D* **39**, 1940 (1989).
  - [14] St. Mrówczyński, *Phys. Lett. B* **314**, 118 (1993); in Proceedings of the International Conference on “Quark Matter ’93,” Borlange, Sweden (in press).
  - [15] St. Mrówczyński, *Phys. Lett. B* **214**, 587 (1988).
  - [16] Yu. E. Pokrovsky and A. V. Selikhov, *Pis'ma Zh. Eksp. Teor. Fiz.* **47**, 11 (1988) [*JETP Lett.* **47**, 12 (1988)]; *Yad. Fiz.* **52**, 229 (1990) [*Sov. J. Nucl. Phys.* **52**, 146 (1990)]; **52**, 605 (1990) [**52**, 385 (1990)]; O. P. Pavlenko, *ibid.* **55**, 2239 (1992) [**55**, 1243 (1992)].
  - [17] M. Gyulassy and A. V. Selikhov, *Phys. Lett. B* **316**, 373 (1993).
  - [18] R. Hwa and K. Kajantie, *Phys. Rev. Lett.* **56**, 696 (1986).
  - [19] T. S. Biró *et al.*, *Phys. Rev. C* **48**, 1275 (1993).
  - [20] K. Eskola and X.-N. Wang, *Phys. Rev. C* **47**, 2329 (1993).